# 4.8 EXTENSION OF THE CPC MJO INDEX TO FORECAST MODE

Qin Zhang
RSIS / Climate Prediction Center / NCEP / NWS / NOAA

Jon Gottschalck and Yan Xue
Climate Prediction Center / NCEP / NWS / NOAA

## 1. BACKGROUND

The Madden-Julian Oscillation (MJO; Madden and Julian 1971, 1972, 1994) is an important mode of weather variability across the global tropics. One of the most noticeable features of the MJO is an eastward progression of large regions of both enhanced and suppressed tropical rainfall, observed mainly over the Indian and Pacific Oceans. In addition, the MJO results in global variations in several other variables including both low- and upper-level wind. The typical length of one MJO cycle is approximately 30-60 days.

In addition to modulating tropical rainfall patterns in general, the MJO has been shown to exert important influences on the extratropical circulation, impact the intensity and onset/decay of monsoon systems, modulate the ENSO cycle, and alter tropical cyclone activity in many ocean basins (Weickmann 1983; Lau and Chan 1985; Higgins et al. 2000, Higgins and Mo 1997, Maloney and Hartmann, 2000a; Maloney and Hartmann, 2000b; Zhang and Gottschalck, 2002). Therefore, it is quite important to monitor and assess the current status of the MJO cycle as it, at times, can play a role in both domestic and international forecasting activities at CPC.

Since 2001, CPC has operationally produced an MJO index using Extended Empirical Orthogonal Function (EEOF) analysis of 200-hPa velocity potential (a measure of upper tropospheric divergence) from the NCEP/NCAR Reanalysis. More details of this technique are outlined in section 2 along with a description of the methodology to produce forecasts of the index. Section 3 summarizes some preliminary findings including initial verification measures and upcoming plans are provided in section 4.

## 2. METHODS

### 2.1 Data and Current Index Methodology

The CPC MJO index is calculated by conducting an EEOF analysis using 200-hPa velocity potential (Xue et al. 2002) from the NCEP/NCAR Reanalysis (Kalnay et al. 1996). The data used in this study are pentad mean 200-hPa velocity potential from 1979 to the present. The velocity potential is a derived quantity, calculated from 200-hPa winds, that isolates the divergent component of the wind at upper levels of the atmosphere. The EEOF analysis was performed on the pentad 200-hPa velocity potential in the tropical region (30°S to 30°N) for lead times from 1 to 10 pentads for both cold and warm seasons. The velocity potential signal related to the interannual signal (ENSO) is addressed by excluding the moderate and strong El Nino (1982/83, 1986/87, 1991/92, 1997/98, 2002/03) and La Nina years (1984/85, 1989/90, 1995/96, 1998/99, 1999/2000). The analysis was performed on the covariance matrix by the square-root of its global mean variance first. Prior to the EEOF analysis, however, we removed the long-term mean and climatological seasonal cycle at each grid-point. The first EEOF mode with ten time lagged patterns obtained from the analysis for both the cold and warm seasons are shown in Figures 1 and 2.

The leading EEOF structure accounts for 16.8% and 16.3% of the total variance of the pentad mean 200-hPa velocity potential field for cold and warm seasons, respectively. The pattern thus describes a large vertically-oriented circulation cell along the equator with upward motion being implied in the region of negative velocity potential anomalies, and downward motion outside that region. The ten lagged spatial patterns represent the MJO propagation for a cycle in the global tropics around 40-45 days. The region of negative velocity potential anomalies in each pattern indicates the location of the enhanced atmospheric deep convection. For example, at time t+20 day in pattern 5 of Figure 1, the strongest convection center (wet phase) is over the Indian Ocean around 80°E. After 5 days, the deep convection shifts to the eastern Indian Ocean around 100°E. Then, it is moving to the Maritime Continent (120°E) at t+30 days and continually propagating eastward to the far western Pacific (140°E) and the western Pacific (160°E) at time t+40 day. Meanwhile, a region of positive velocity potential anomaly follows behind the deep convection at t+45 day with less precipitation (dry phase) over the Indian Ocean and then propagates eastward. The convection center moves eastward continually and returns to Africa after 40 or 45 days. The intensity of the MJO both wet and dry phases enhance over the Indian Ocean and the western pacific and reduce when they move into the eastern Pacific and Atlantic. The MJO propagation varies with a slower speed over the Indian Ocean and the western Pacific but faster speed over the eastern

pacific and Atlantic and Africa. The MJO reinitializes over the Africa continents after 40-45 days.

The second EOF structure, on the other hand, accounts for 16.7% and 16.5% of the total variance for cold and warm seasons, with it being approximately in quadrature with the first. Together the EEOFs form a degenerate pair, and they can represent the spatially propagating signal of the MJO. Ten MJO indices are calculated by projecting the observed pentad velocity potential data onto the previously described EEOFs time series and these indices can be used in realtime.

Figure 3 is an example of the calculated MJO indices for 2002. The negative values indicate the enhanced phase of the MJO while positive values indicate the suppressed phase of the MJO. For real time monitoring, the MJO indices based on the above methodology are used in conjunction with daily 200-hPa velocity potential and determine daily values of the ten MJO indices and are displayed in time-longitude format so as to reveal the propagation, amplitude and location of the MJO if it is active.

### 2.2 Forecast Model

The CPC MJO indices as described in section 2 have been extended to forecast mode by applying a Markov modeling approach. As in Xue et al (2000), we construct Markov model in a two step EOF analysis. The first step is decomposing 200hPa velocity potential anomalies into EEOFs ($E_j$, spatial patterns) and their corresponding PCs ($P_j(t)$, time series) for space reduction. Combining the ten spatial patterns into a single vector $V(t)$ , we have:

$$V(t) = \sum_{j=1}^{J} P_j(t) E_j \qquad (1)$$

The Markov model is computed using the single-step correlation matrix, that is, a transition matrix A that satisfies the linear relation,

$$P_j(t+1) = AP_j(t) + \varepsilon_j, \qquad (2)$$

where ε is the error in the model fit.

The model given in (2) is trained using 200hPa velocity potential data for the period from 1979-2004. Forecast models are developed for cold and warm seasons, separately. The spatial structures are obtained by reconstructing the field of 200hPa velocity potential using the PC forecasts. For example, for one time step of forecast PC's, ten patterns of 200-hPa velocity potential anomalies are obtained by projection. Since the ten patterns that represent the MJO wave propagation in the next 10 pentads are also arranged in successive time as indicated in Figure 1, the forecasts are duplicated.

## 3. INITIAL RESULTS

### 3.1. MJO Composites

Due to the slowly evolving nature of the MJO, accurate prediction is fundamentally related to our ability to monitor and assess its relative position and strength. Consequently, composites can be a very useful tool for both monitoring and forecasting applications as they address typical impacts in important quantities by MJO phase. In order to calculate composites, we defined eight phases of the MJO for both cold and warm seasons according to the values of PC1 and PC2 described above. In the two-dimensional phase space of PC1 and PC2 of the EEOF of the 200hPa velocity potential anomalies we only chose those cases in which the amplitude of PC1 and PC2 is greater than 1. Keying on the convectively active phases of the MJO, eight phases of a composite MJO are constructed for various fields that include OLR, precipitation, and 500hPa height anomalies. Only areas significant at the 95% confidence interval are shaded in the composites (Figure 5 a-b). For the cold season OLR composite, as an example, the areas of enhanced convection clearly show the eastward propagation of the MJO starting with phase 1 which shows enhanced convection in the Africa region.

### 3.2 MJO Forecast and Verification

Forecasts of the CPC MJO indices derived from 200-hPa velocity potential using the Markov model are presented here. Figure 5 shows the one pentad leading forecast of the CPC MJO indices from the Markov model in 2002 with prediction initiated from the same time as in Figure 3. Overall, the pattern correlation of the forecast with the observed indices in 2002 is 0.74. The speed of the eastward propagation is very similar to the observations. The forecasts of the CPC MJO indices for the strong MJO that occurred during April to July and again during October to December match reasonably well with the observations. The weak MJO activity in the beginning and summer of the 2002 time period illustrate considerable differences across the central Pacific. The results indicate that the statistical forecast of the CPC MJO indices have high skill when an MJO event has already started, i.e. enhanced convective activity is fully developed over the tropical Indian Ocean and is propagating eastward towards Indonesia and is typical

of most statistical MJO forecasting methods. The verification of the forecast for 200hPa velocity potential is presented in terms of pattern (spatial) correlation between forecast and observation. The cross-validated skill for 1979-2004 time period is currently being evaluated.

## 4. SUMMARY AND UPCOMING PLANS

The current CPC MJO index (based on EEOF analysis of 200-hPa velocity potential) has been produced operationally for several years and has proven to be a useful tool for monitoring and assessing the current status of the MJO cycle in realtime. In the past, the index has been most applicable to describe the temporal evolution of the MJO for the Northern Hemisphere cold season. In this paper, we describe work that applies this technique to the Northern Hemisphere summer season and the extension of the MJO index to operate in a forecast mode using a linear Markov model methodology. The preliminary results are encouraging and warrant further evaluation of this methodology for MJO monitoring and forecast. The predicted CPC MJO indices catch the features of eastward propagation and phase change very well. The forecast skill is relative high over the Indian Ocean and the western Pacific. The described approach in this paper may provide an important complement to other techniques currently utilized at CPC as part of the MJO weekly update and experimental global tropics benefits/hazards assessment under development at CPC.

For future work, we are planning to compare the Markov model forecast with other statistical and dynamical forecast models including the Global Forecast System (GFS) from NCEP. Multivariate approaches will be considered to train a new Markov model for direct prediction of the MJO and related precipitation. Also, different methods for removing the ENSO signal will be tested for better suitable for the realtime MJO monitoring and forecast.

## REFERENCES


Higgins, R. W., and K. C. Mo, 1997: Persistent North Pacific circulation anomalies and the tropical intraseasonal oscillation. J. Climate, 10, 223-244.

Kalnay, E., and co-authors, 1996: The NCEP/NCAR Reanalysis Project. *Bull. Amer. Meteor. Soc.*, **77**, 437-471.

Lau, K-M, and P. H. Chan, 1985: Aspects of the 40-50 day oscillation during the northern winter as inferred from outgoing longwave radiation. *Mon. Wea. Rev.*, 113, 1889-1909.

Madden, R and P. R. Julian, 1971: Detection of a 40-50 day oscillation in the zonal wind in the tropical Pacific. *J. Atmos. Sci.*, 28, 702-708.

Madden, R, and P. R. Julian, 1972: Description of global-scale circulation cells in the tropics with 40-50 day period. *J. Atmos. Sci.*, 29, 1109-1123.

Madden, R, and P. R. Julian, 1994: Observations of the 40-50 day tropical oscillation - A review. *Mon. Wea. Rev.*, 122, 814-837.

Maloney, E. D. and D. Hartmann, 2000a: Modulation of eastern North Pacific hurricanes by the Madden-Julian Oscillation. *J. Climate*, 13, 1451-1460.

Maloney, E. D. and D. Hartmann, 2000b: Modulation of hurricane activity in the Gulf of Mexico by the Madden-Julian Oscillation. *Science*, 287, 2002-2004.

Weickmann, K. M., 1983: Intraseasonal circulation and outgoing longwave radiation modes during the Northern Hemisphere winter. *Mon. Wea. Rev.*, 111, 1838-1858.

Xue, Y, A. Leetmaa, and M. Ji, 2000: ENSO prediction with Markov models: The impact of sea level. *J. Climate*, 13, 849-871.

Xue, Yan, R. W. Higgins, H.-K. Kim and V. Kousky, 2002: Impacts of the Madden Julian Oscillation on U.S. Temperature and Precipitation during ENSO-Neutral and Weak ENSO Winters. 26th Climate Diagnostics and Prediction Workshop. [Available at http://www.cpc.ncep.noaa.gov/products/outreach/CDW26.html]

Zhang, C. and J. Gottschalck, 2002: SST Anomalies of ENSO and the Madden-Julian Oscillation in the Equatorial Pacific. *Journal of Climate*, 15, 2429-2445.

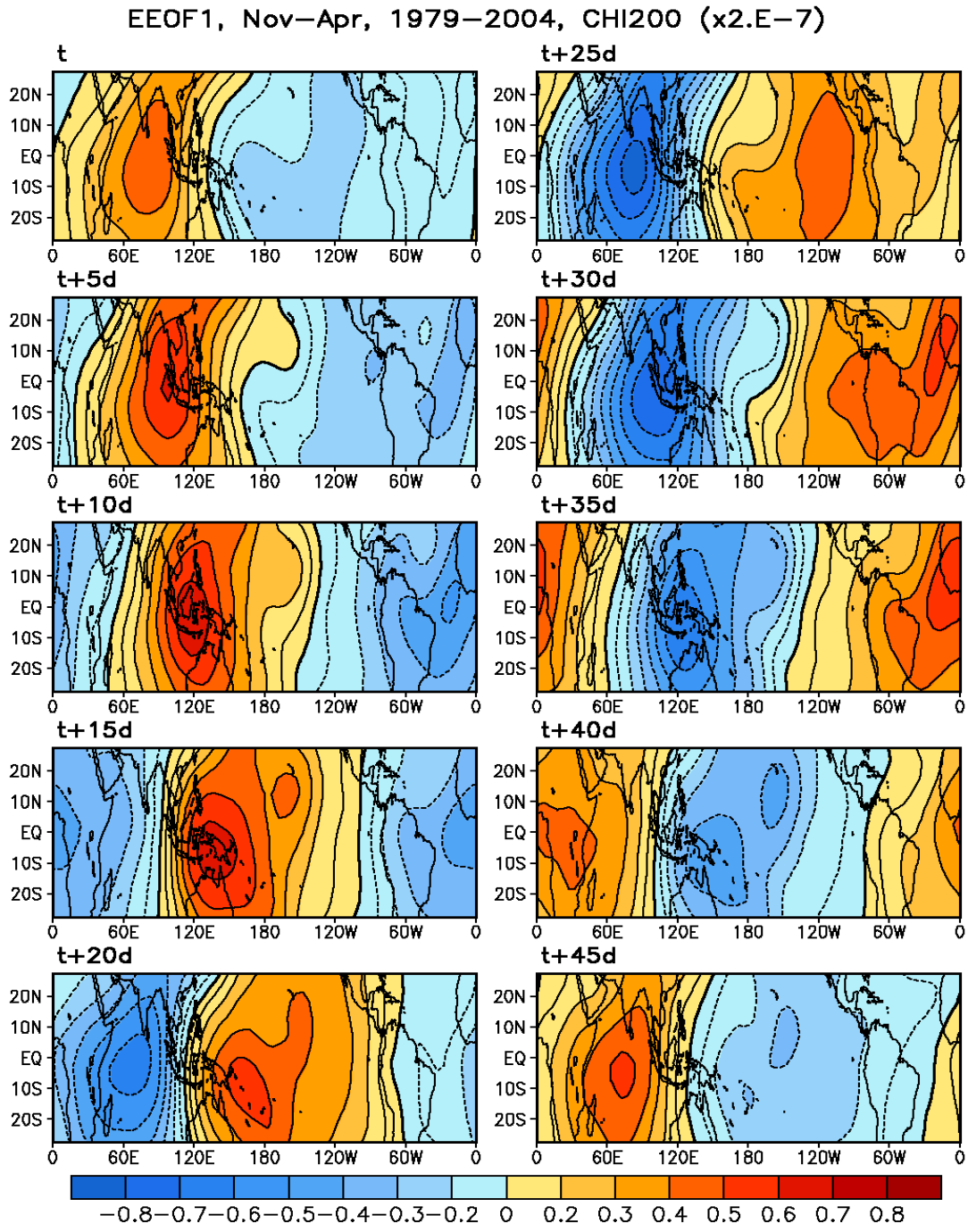


Figure 1: The first EEOF mode of 200-hPa velocity potential anomaly with ten pentad time lags for cold season. The blue shadings indicate the location of the enhanced atmospheric deep convection. (cint: $2*10^{-7}$ $ms^{-1}$)

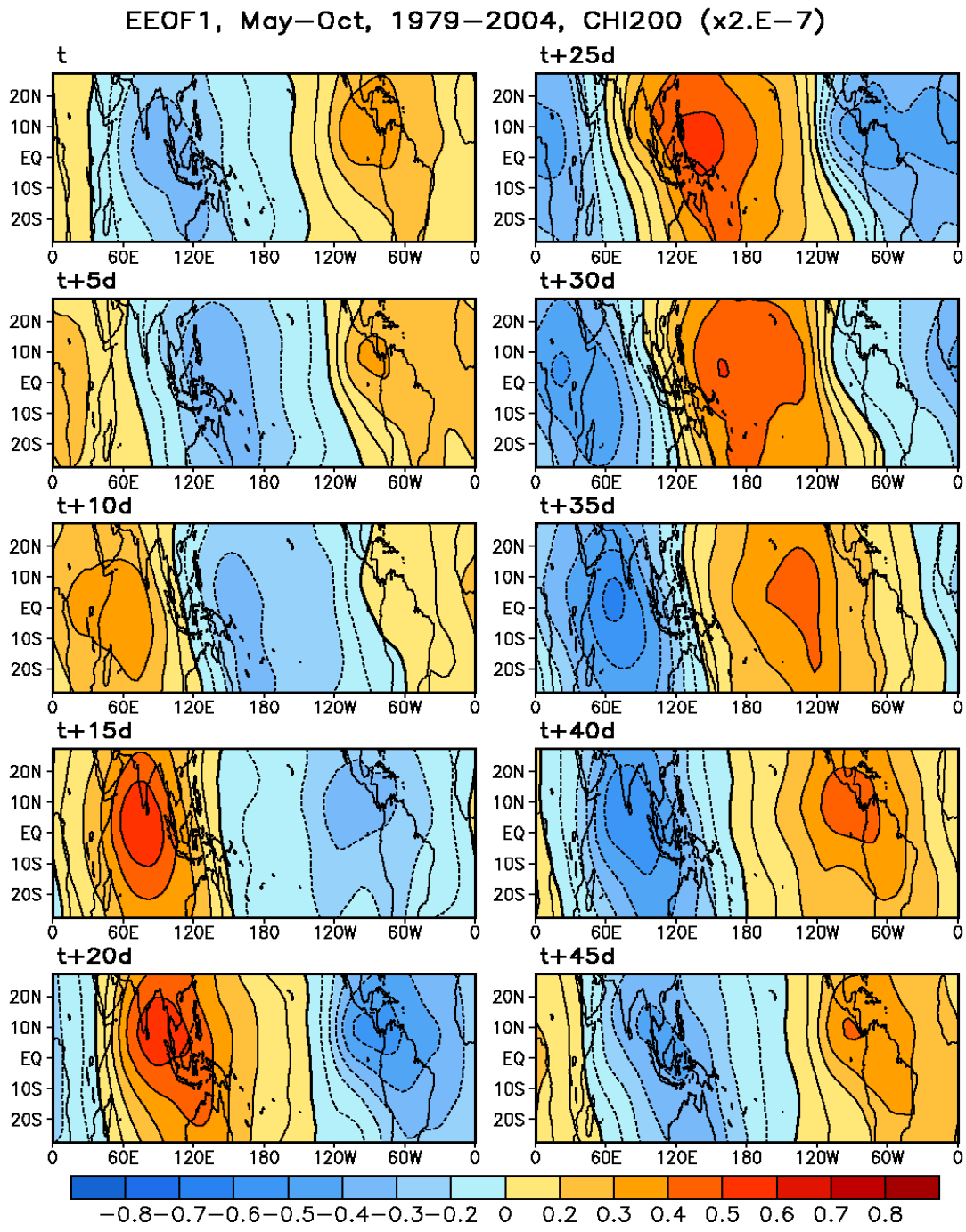


Figure 2: Same as Figure 1 except for warm season.

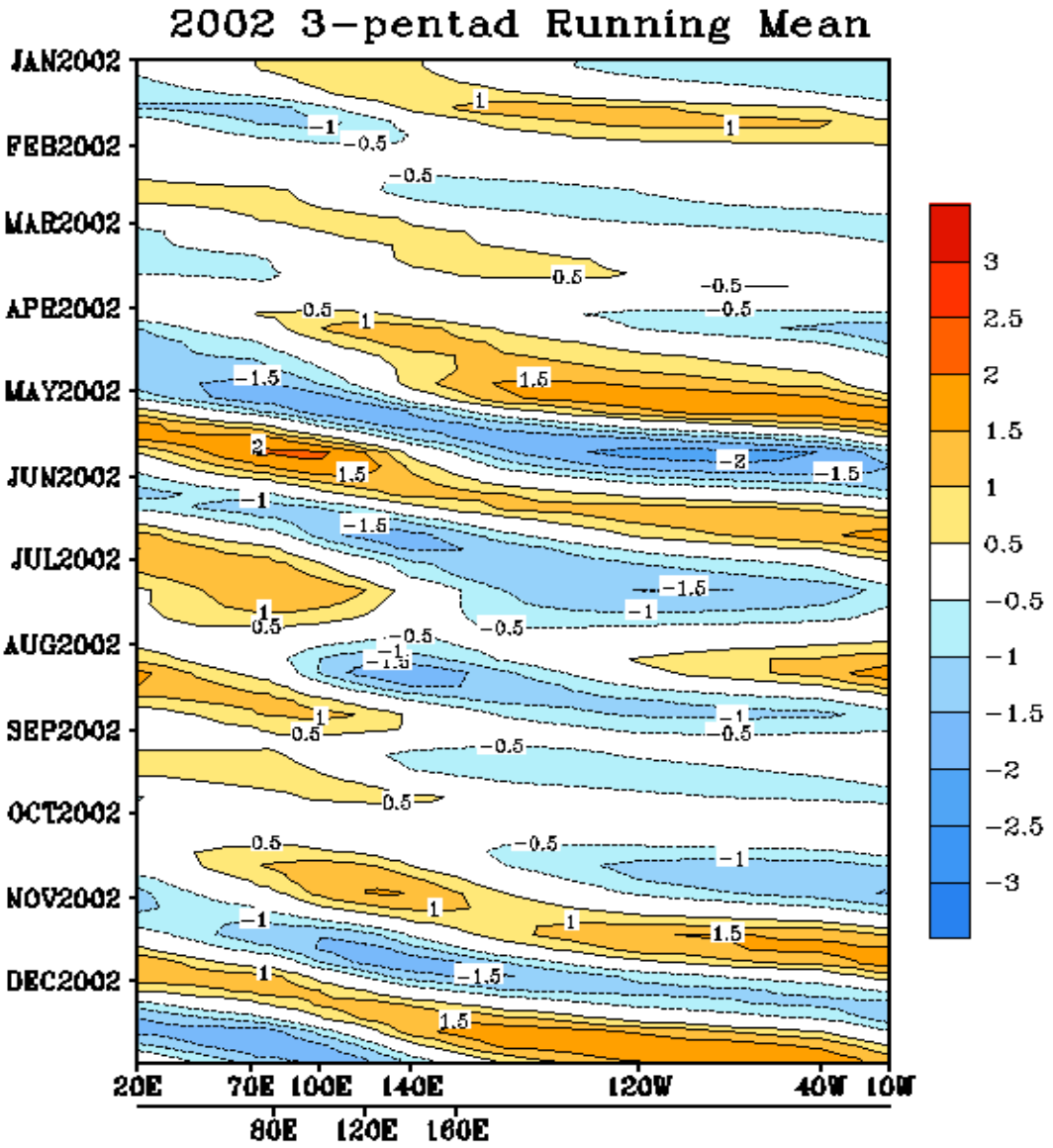


Figure 3: Pentad mean CPC MJO indices for 2002. The negative values represent the MJO related convection center propagation eastward. The values are normalized.

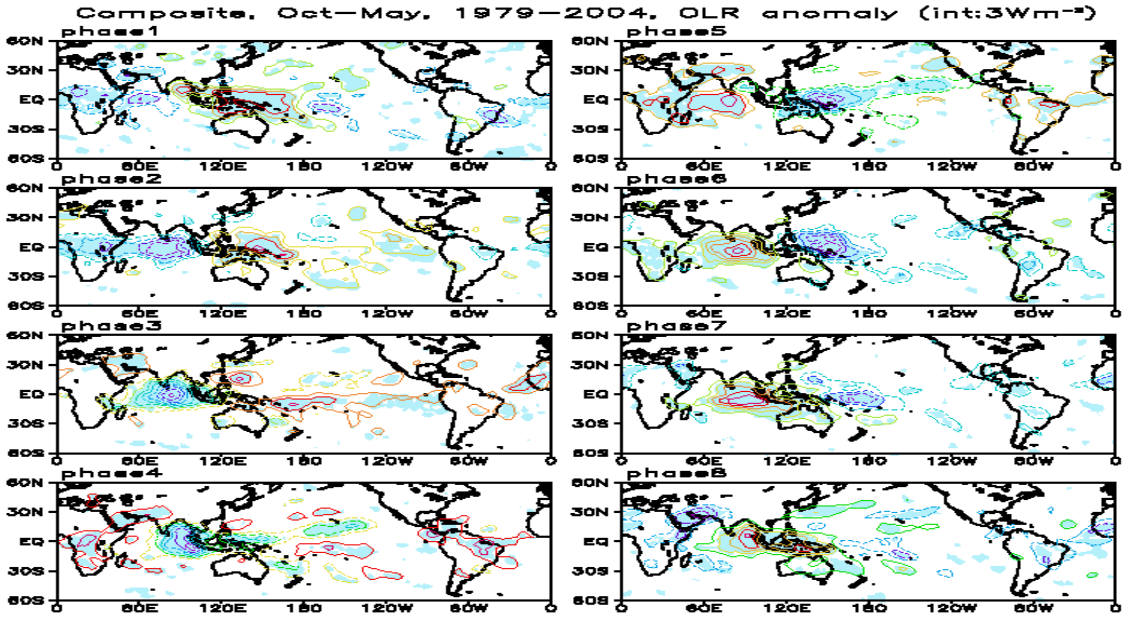


Figure 4: (a) OLR MJO composites for the eight phases of MJO for the cold season. Blue dashed contours indicate the deep convection centers. The shadings are the regions of significant at the 95% confidence of t-test. (cint: 3 Wm-2)

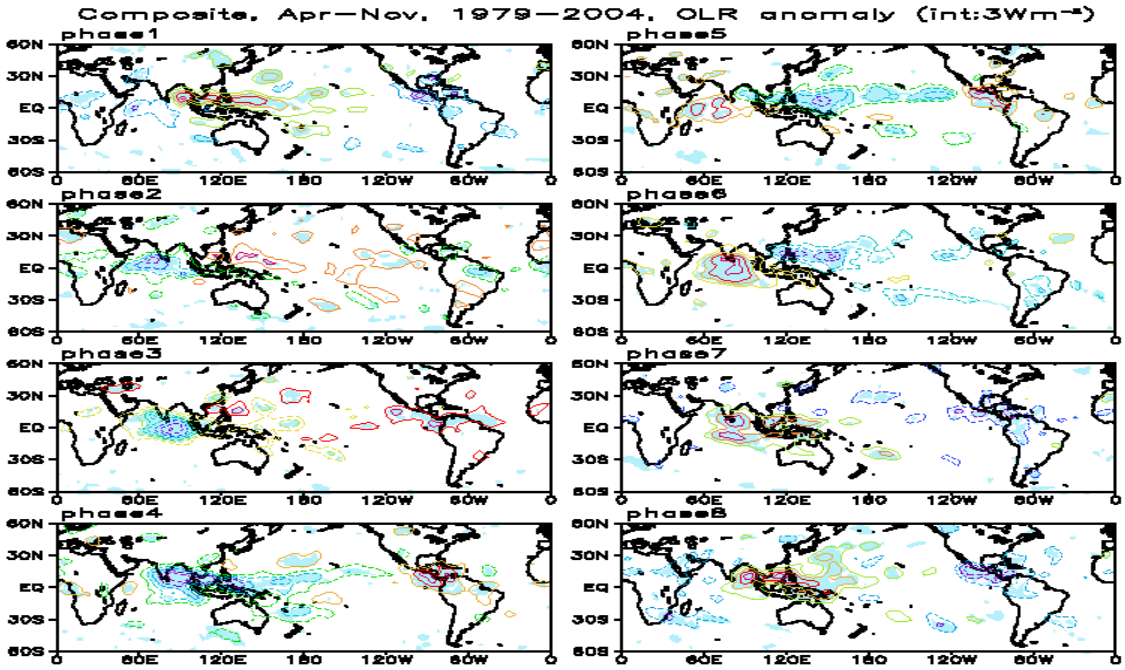


Figure 4: (b) Same as Fig. 4 (a) except for warm season.

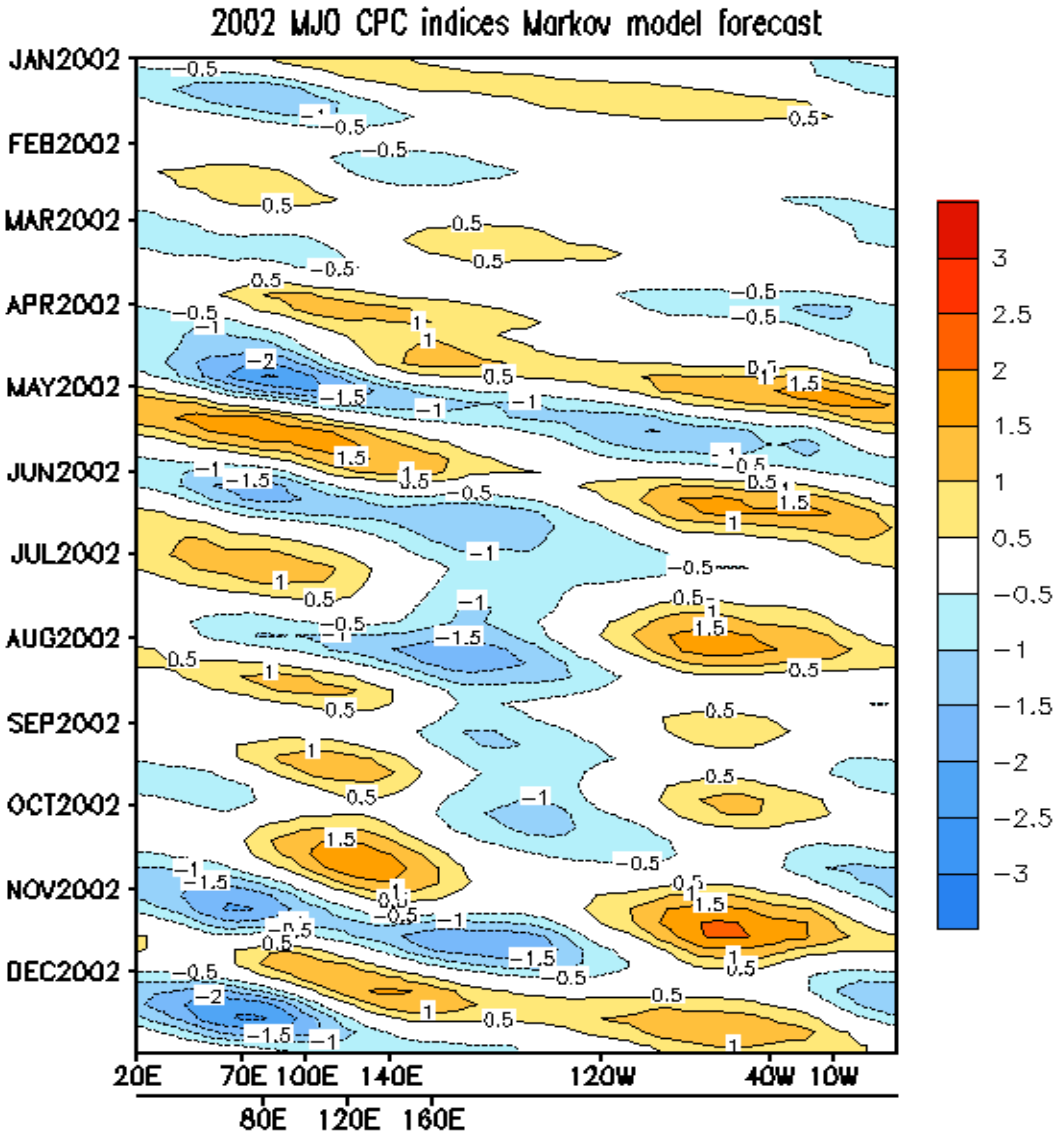


Figure 5: Prediction of the CPC MJO indices by Markov model for 2002. The negative values represent the MJO related convection center propagation eastward. The values are normalized.